

Analysis of L-type calcium channel block by trivalent ions: Gd³⁺ competes with permeant ions for the selectivity filter

Attila Malasics¹, Dezsó Boda^{1,2}, Mónika Valiskó¹, Douglas Henderson², and Dirk Gillespie^{3,*}

¹Department of Physical Chemistry, University of Pannonia, Veszprém, Hungary

²Department of Chemistry and Biochemistry, Brigham Young University, Provo, Utah

³Department of Molecular Biophysics and Physiology, Rush University Medical Center,
Chicago, Illinois

*corresponding author: 1750 W. Harrison St. Suite 1289, Chicago, IL 60612, (312) 942-3089,
fax: (312) 942-8711, dirk_gillespie@rush.edu

keywords: L-type calcium channel, dihydropyridine receptor, tonic block, permeation, selectivity

30 October 2009

ABSTRACT

Current through L-type calcium channels ($\text{Ca}_v1.2$ or dihydropyridine receptor) can be blocked by micromolar concentrations of trivalent cations like the lanthanide gadolinium (Gd^{3+}). These cations seem to affect both ion permeation and pore gating. One effect of trivalents is that the whole-cell peak current recorded after a conditioning voltage pulse depends on $[\text{Gd}^{3+}]$, a phenomenon called tonic block. Recently, Babich et al. (*J. Gen. Physiol.* 129 (2007) 461-475) proposed that tonic block is due to ions competing for a binding site when the channel is closed, and when the channel opens, Gd^{3+} blocks the pore to prevent the conduction of other ions; tonic block is not due to changes in gating properties, but reflects only permeation. Here, we corroborate this view by computing conductance in a model L-type calcium channel. The model not only reproduces the Gd^{3+} concentration dependence of the current reduction, but also the effect that substantially more Gd^{3+} is required to produce similar block in the presence of Sr^{2+} (compared to Ba^{2+}) and even more in the presence of Ca^{2+} . Tonic block is explained in this model by cations binding in the selectivity filter with the charge/space competition mechanism. In this mechanism, selectivity is determined by the combination of ions that most effectively screen the negative glutamates of the protein while finding space in the midst of the closely-packed carboxylate groups of the glutamate residues.

INTRODUCTION

L-type calcium channels ($\text{Ca}_v1.2$) have an extremely high affinity for divalent cations like Ca^{2+} , Sr^{2+} , and Ba^{2+} . Even at micromolar concentrations these ions can occupy and block the pore often enough to significantly reduce monovalent cation current [1, 2]. However, these divalents are conducted by the pore and therefore the channel is never completely blocked (i.e., current is never zero, no matter how large the concentration of divalents). The story is different for trivalent cations like the lanthanide gadolinium (Gd^{3+}). These can completely block the current through an open channel at concentrations $<10 \mu\text{M}$ [3-6].

Identifying the mechanism by which trivalents reduce the permeation of ions through an open channel is challenging because the trivalents affect the gating of L-type [3] and T-type [7] calcium channels by accelerating current decay during depolarization. This so-called “use-

dependent block” is the decrease of peak currents in whole-cell recordings after two voltage pulses in the presence of trivalent cations. That is, the peak current during the second pulse (I_2) is less than the peak current during the first pulse (I_1), and the ratio I_2/I_1 is extremely sensitive to the trivalent concentration [5]. The peak current after the first pulse (I_1) also decreases as trivalent concentration increases [5]. This is referred to as “tonic block.”

While use-dependent block has time-dependent aspects that suggest changes in gating caused by the trivalents, it is not known the extent tonic block involves changes in permeation and changes in open probability. Recently, Babich et al. [5] proposed that Gd^{3+} causes both tonic and use-dependent block by binding to an extracellular binding site at the mouth of the selectivity filter. In their view, the site is accessible when the channel is closed and both Gd^{3+} and the permeant ions compete for the site (which has a higher affinity for Gd^{3+}). Tonic block then reflects Gd^{3+} block of the permeation pathway after the channel opens. Use-dependent block is a subsequent process that involves conformational changes.

In this paper we analyze this picture of tonic block. To do this we use a model of the L-type calcium channel to compute the conductance of the channel in the presence of Gd^{3+} . We find that the concentration dependence of tonic block is well reproduced with the model pore by the competitive binding of Gd^{3+} and the permeant cations in the selectivity filter. This is consistent with Babich et al. and indicates that tonic block probably represents the block of open-channel current by Gd^{3+} . We do, however, differ with Babich et al. about the location of the binding site. In their view the location is probably adjacent to the selectivity filter on the extracellular side, whereas in the model the location is the selectivity filter itself.

This difference may be attributed to the very different models used here and by Babich et al. They used a chemical kinetic scheme that has commonly been used for these kinds of calcium channels (and criticized [8-11]). We use a very different approach. Our model of the pore assumes only that the selectivity filter of the L-type channel is the bottleneck for ion permeation and that the filter is a cluster of four flexible glutamate residues that move freely within the filter to coordinate the cations. Selectivity occurs because cations are electrostatically attracted to the negatively charged pore and the ions must find space within the crowded selectivity filter where much of the available space is taken up by the side chains of the four glutamates. This very reduced model has successfully reproduced both the conductance and selectivity properties of the L-type channel, including micromolar Ca^{2+} block of Na^+ current,

anomalous mole fraction effects in mixtures of Ca^{2+} and Ba^{2+} , and selectivity in other ion mixtures [12-15]. While this approach does not explain specific contributions for the individual glutamates or the role of nonglutamate residues, it does provide an intuitive, leading-order interpretation of permeation and selectivity. Additional atomic details will refine the results of this model, but not change its big-picture findings because those details will only tweak the leading-order physics. Moreover, a similar reduced model has correctly reproduced all the permeation and selectivity data—as well as predicting other, counterintuitive data—of the ryanodine receptor calcium channel [16-19].

In this paper we find that Gd^{3+} binds in the selectivity filter, competing with other permeant ions. Without any adjustable parameters, this competitive binding reproduces the Gd^{3+} concentration dependence of tonic block measured by Babich et al. [5]. Specifically, they measured tonic block in mixtures of 150 mM Na^+ , 10 mM divalent (Ca^{2+} , Sr^{2+} , or Ba^{2+}), and varying amounts of Gd^{3+} (0.001 to 10 μM), conditions that are challenging for any model because three cations are competing for the pore. Still the model naturally explains the differences observed when different divalents compete with Gd^{3+} . Collectively, the lack of adjustable parameters, the complexity of three cations competing for the pore, and the large range of Gd^{3+} concentrations give us confidence that this model explains the big-picture features of tonic block. Unfortunately, we cannot make any assessments of use-dependent block because the model is of an open pore only and does not include gating.

THEORY AND METHODS

Model of the L-type calcium channel

The model of the L-type calcium channel pore is the simplest possible: a selectivity filter between two uncharged vestibules that connects two baths. This is shown in Fig. 1. The selectivity filter is a hard cylinder that is 10 Å in length and 3.5 Å in radius. It contains the four glutamates that produce the selectivity of this channel [20, 21]. We model each of these as only their negatively charged terminal carboxyl (COO^-) group, and each of these as two half-charged, independent oxygens ($\text{O}^{1/2-}$). The glutamates face the permeation pathway and the carboxyl groups are probably relatively free to move within the filter, but are tethered to the protein by the CH_2 groups of the side chain. We model this freedom of movement with infinite flexibility: the eight oxygens are free to move anywhere within the selectivity filter cylinder, but cannot leave

the cylinder. Except for that constraint, the oxygens are subject to all the same forces as all the permeating ions, namely thermal motion, Coulombic interactions, and dispersion forces.

The dispersion forces are modeled very crudely by having all the particles (oxygens, Cl^- , and permeant cations) be charged, hard spheres. Therefore any two particles interact Coulombically and they cannot overlap. The size of each hard sphere is the Pauling radius: Na^+ 0.95 Å, Ca^{2+} 0.99 Å, Sr^{2+} 1.13 Å, Ba^{2+} 1.35 Å, Gd^{3+} 0.94 Å, Cl^- 1.81 Å, and $\text{O}^{1/2-}$ 1.40 Å.

The particles also interact electrostatically with the pore itself. Specifically, the dielectric constant of the protein is different from that of the permeation pathway (10 and 80, respectively) so that the ions induce a surface charge on this dielectric interface (image charges). Each ion induces charges that would normally repel it from the pore. This approximates the dehydration energy needed for the ion to strip waters off to enter the pore. However, cations go into the pore because not only are there four negative glutamates to draw them in, but also because of the negative induced charges of these glutamates; the low dielectric constant of the protein helps to amplify the negative structural charge of the pore [12, 22].

The details of the model pore have been described previously [13, 15].

Computing conductance

The Monte Carlo (MC) simulations that we use (described below) are designed for equilibrium. Therefore, we have two identical baths and no applied voltage. From this situation it is still possible to compute the conductance at zero applied voltage V because, while the current I is zero, the slope conductance dI/dV is not. To compute conductance, we start with the Nernst-Planck (drift-diffusion) equation [13, 19]. In three dimensions, this is

$$-\mathbf{J}_i(\mathbf{x}) = \frac{1}{kT} D_i(\mathbf{x}) \rho_i(\mathbf{x}) \nabla \mu_i(\mathbf{x}) \quad (1)$$

where, for ion species i , $\mathbf{J}_i(\mathbf{x})$ is the flux per unit area, $D_i(\mathbf{x})$ is the diffusion coefficient profile from the bath through the pore, $\rho_i(\mathbf{x})$ is the density profile, and $\mu_i(\mathbf{x})$ is the electrochemical potential profile. The Boltzmann constant is k and the absolute temperature is T .

As before with this model pore, we assume that the flux is limited only in the selectivity filter (the cylindrical part of our pore) [13, 15]. It has previously been shown that, when a very small driving force is applied, Eq. (1) can be integrated to give the conductance γ at zero voltage [15]:

$$\gamma = \frac{1}{kT} \sum_i D_i z_i^2 e_0^2 \left(\int \frac{dz}{n_i(z)} \right)^{-1} \quad (2)$$

where $n_i(z)$ is the axial number density of ions (i.e., the number of ions of species i in a slice of the pore of width dz centered around axial location z). We take the diffusion constant in the cylinder D_i to be constant in both the axial and radial directions. The valence of species i is z_i and e_0 is the fundamental charge. For the ions we consider here, the normalized conductance is given by

$$\frac{\gamma}{\gamma^0} = \frac{\frac{D_{\text{Gd}}}{D_{\text{Na}}} \eta_{\text{Gd}} + \frac{D_{\text{M}}}{D_{\text{Na}}} \eta_{\text{M}} + \eta_{\text{Na}}}{\frac{D_{\text{M}}}{D_{\text{Na}}} \eta_{\text{M}}^0 + \eta_{\text{Na}}^0} \quad (3)$$

where

$$\eta_i = z_i^2 e_0^2 \left(\int \frac{dz}{n_i(z)} \right)^{-1} \quad (4)$$

and the conductance has been normalized with that in the absence of Gd^{3+} (denoted by the 0 superscript).

It is important to note that Eq. (2) is only valid for a small voltage range around zero where the current/voltage curve is linear. Technical details regarding the validity of using the Nernst-Planck equation in this pore have been described previously [13].

Monte Carlo simulations

The conductance, as computed from Eq. (2), requires the line density profile $n_i(z)$ as an input. We use Metropolis MC simulations to compute this profile. The details of the simulations have been described previously [14, 22, 23] and we only review them briefly here.

The Gd^{3+} experiments require very low bath concentrations (e.g., 10^{-8} M). These very low concentrations can be achieved in the MC simulations by performing these simulations in the grand canonical ensemble where the bath chemical potential is held fixed, rather than the number of particles in the simulation cell. Because of this, ions are created or deleted (see below) and the average number of ions of one species in the simulation cell can be less than 1. The chemical potentials that make the desired bath concentrations were computed in a separate grand canonical ensemble simulation as described previously [24].

In MC, one ion (permeating, as well as oxygens and Cl^-) at a time is picked at random and moved to a random (although possibly biased) new location. The energy change of this

move is computed and a move is accepted with a probability that ensures microscopic reversibility. Possible moves include: (1) small changes from the old position (for sampling of regions with high densities like the selectivity filter where $\sim 25\%$ of the available space is taken up by oxygens); (2) changes to a new position selected randomly from a uniform distribution anywhere in the cell (for sampling regions with low densities like the baths where the ions have gas densities because of our implicit-solvent model of the electrolyte); (3) moving a particle from a position in the selectivity filter to a position in the baths (or vice versa), a preferential move between subvolumes needed to efficiently sample the pore that takes up only a small fraction of the volume of the simulation cell [23]; (4) insertion or removal of a neutral group of ions (e.g., $\text{Na}^+ + \text{Cl}^-$ or $\text{Ca}^{2+} + 2\text{Cl}^-$) into or from the simulation cell; and (5) cation insertions or deletions analogous to (4) but directly into or out of the selectivity filter [14] with anions inserted or deleted from the baths. Moves (3), (4), and (5) are necessary in order to have enough configurations with ions at low bath densities (e.g., Gd^{3+}).

The results presented here are averages of many simulations performed on multiple processors and with different starting configurations. In total, 6×10^8 to 1.2×10^9 MC moves are attempted for each result we present.

A successful reduced model

This model obviously excludes most the structural details one might deem important. Nevertheless, it seems to capture the essential physics of selectivity of the L-type channel. For example, without adjustable parameters like diffusion coefficients it naturally has micromolar Ca^{2+} affinity. It also reproduces the classical anomalous mole fraction effect of Almers and McCleskey [1, 2]—the only model of this channel to have done so with direct simulations of micromolar $[\text{Ca}^{2+}]$ [13]. Without changing anything about the structure of the pore, it also reproduces the L-type channel's size selectivity properties (i.e., selectivity among ions of the same charge) in mole fraction [13] and added- Ca^{2+} [15] mixtures of Ca^{2+} and Ba^{2+} , as well as mole fraction mixtures of Li^+ and Na^+ [15].

The reason for this success is probably that the physics of these phenomena is dominated by electrostatics and dispersion forces (i.e., the excluded volume of the ions forcing them not to overlap), the two forces explicitly included in the model. In that case one would not expect that the details of the arrangement of the amino acids matters, at least to first order. These details do

matter for other experimental data that this model fails to reproduce (e.g., that mutating each of the four glutamates does not produce identical results [20]).

The data that we analyze in this paper (i.e., how Na^+ , divalents, and Gd^{3+} competitively bind in the selectivity filter) is the type of data that this model has reproduced well. We do not change any of the parameters of the pore (e.g., radius, length, dielectric coefficients) from previous papers and the ion sizes are fixed to be Pauling radii. Therefore, the results we show are what comes out of the model pore naturally. If the model did not include the correct physics to describe this process (either in the ion binding or in the conductance), the results would most likely be incorrect since we are attempting to reproduce data over a large range (e.g., four orders of magnitude of Gd^{3+} concentration) and since this problem is particularly challenging with three cations competing for the pore.

RESULTS

Computing the tonic block experiments

Babich et al. [5] measured the Gd^{3+} dependence of tonic block in asymmetric solutions. The internal solution contained 155 mM CsCl, 10 HEPES, and 5 mM Mg-ATP, while the extracellular solution contained 150 mM NaCl, 10 mM Tris-Cl, and 10 mM CaCl_2 , SrCl_2 , or BaCl_2 . Gd^{3+} was added to the extracellular side. The MC simulation method is designed for symmetric solutions, so we performed the simulations in symmetric 150 mM NaCl, 10 mM CaCl_2 , SrCl_2 , or BaCl_2 , and the indicated concentration of Gd^{3+} . This difference in protocol is not expected to qualitatively affect the general conclusions because the applied voltage in the experiments moved extracellular cations inward, as we have found in previous studies [13, 15].

The comparisons of our calculations of normalized conductance to the experimental values are shown in Fig. 2. Like the experimental results, each conductance γ is normalized to the conductance in the absence of Gd^{3+} (γ^0). The model reproduces the differential effect of Gd^{3+} on Ca^{2+} , Sr^{2+} , and Ba^{2+} qualitatively: Ba^{2+} is initially affected by $\sim 0.01 \mu\text{M}$ Gd^{3+} , Sr^{2+} requires more Gd^{3+} to see an effect, and Ca^{2+} requires even more.

The model results are, of course, not perfect. Fitting the model results with the equation

$$\frac{\gamma}{\gamma^0} = \frac{1}{1 + \frac{[\text{Gd}^{3+}]}{\text{IC}_{50}}}, \quad (5)$$

we computed IC_{50} 's for Gd^{3+} in the presence of the divalents (experimental results [5] are in parentheses): for Ca^{2+} , $IC_{50} = 1.6 \pm 0.08 \mu M$ (0.29 ± 0.05); for Sr^{2+} , $0.44 \pm 0.03 \mu M$ (0.12 ± 0.02); for Ba^{2+} , $0.045 \pm 0.003 \mu M$ (0.03 ± 0.01). While the IC_{50} for Ba^{2+} is close to the experimental value, the IC_{50} 's for Sr^{2+} and Ca^{2+} are too large by factors of 3.7 and 5.3, respectively.

However, given the evident structural differences between our very reduced model of the pore and the real channel, this agreement is remarkable; the model includes the simplification of four indistinguishable glutamates of the selectivity filter [20], only approximately takes ion dehydration into account, and uses symmetric ion solutions instead of the real experimental conditions. The experimental difficulties of working with Gd^{3+} also cannot be overlooked. For example, to avoid using buffers (which cause their own difficulties [15]) 1 mM $GdCl_3$ solutions had to be diluted down to 10 nM. Babich et al. also describe that just switching from glass to polycarbonate containers affected the measurements with “dramatically improved consistency of results at $[Gd^{3+}] < 1 \mu M$ ” [5].

Most model results are independent of unknown parameters

One significant (and unexpected) aspect of the normalized conductances in Fig. 2 is that they are independent of the ion diffusion coefficient ratios of Eq. (3). Whereas ion diameters can be estimated with Pauling diameters and the pore parameters (e.g., protein dielectric coefficient and pore radius) can be estimated by matching the experimentally-determined micromolar Ca^{2+} affinity [12], ion diffusion coefficients are the only parameters for which we do not have reliable independent estimates.

The fact that the conductances are independent of the diffusion coefficient ratios comes from two findings:

1. the conductance of Gd^{3+} is always zero because $n_{Gd}(z) \approx 0$ outside the center of the selectivity filter (see Fig. 5 later) and therefore $\eta_{Gd} = 0$ (Eq. (4));
2. the concentration profiles $n_i(z)$ of Na^+ and the divalents M^{2+} change in the same proportion with varied $[Gd^{3+}]$. That is,

$$\frac{n_M(z)}{n_{Na}(z)} = \frac{n_M^0(z)}{n_{Na}^0(z)} \quad (6)$$

where the function $n_i(z)$ is the line density from Eq. (2) (which depends on $[\text{Gd}^{3+}]$) and the superscript 0 refers to the profile when $[\text{Gd}^{3+}] = 0$. This is shown in Fig. 3. Because of Eq. (6) and because the conductance of Gd^{3+} is zero, Eq. (3) becomes

$$\begin{aligned} \frac{\gamma([\text{Gd}^{3+}])}{\gamma^0} &\approx \frac{\frac{D_M}{D_{\text{Na}}} \eta_M([\text{Gd}^{3+}]) + \eta_{\text{Na}}([\text{Gd}^{3+}])}{\frac{D_M}{D_{\text{Na}}} \eta_M^0 + \eta_{\text{Na}}^0} \\ &= \frac{\eta_{\text{Na}}([\text{Gd}^{3+}])}{\eta_{\text{Na}}^0} = \frac{\eta_M([\text{Gd}^{3+}])}{\eta_M^0}. \end{aligned} \quad (7)$$

The consequence of the normalized conductance being independent of the diffusion coefficient ratios is that the normalized pore conductance γ / γ^0 is determined solely by the ion binding selectivity properties of the model pore through the density profiles $n_i(z)$ in η_i (Eq. (4)). (Of course the absolute conductance γ does depend on the diffusion coefficients.) The model results are then more robust, in that they are not subject to particular choices of parameters that are difficult to estimate independently.

This is not to say that—with an educated estimate—insight cannot be gained by analyzing quantities that do depend on the diffusion coefficients. For example, consider the individual Ca^{2+} and Na^+ conductances. In Fig. 4 we plot these, normalized to the total conductance in the absence of Gd^{3+} . For Ca^{2+} this is (by Eq. (3))

$$\frac{D_{\text{Ca}} \eta_{\text{Ca}}}{D_{\text{Ca}} \eta_M^0 + D_{\text{Na}} \eta_{\text{Na}}^0} = \frac{\frac{D_{\text{Ca}}}{D_{\text{Na}}} \eta_{\text{Ca}}}{\frac{D_{\text{Ca}}}{D_{\text{Na}}} \eta_M^0 + \eta_{\text{Na}}^0} \quad (8)$$

and for Na^+ conductance it is

$$\frac{D_{\text{Na}} \eta_{\text{Na}}}{D_{\text{Ca}} \eta_M^0 + D_{\text{Na}} \eta_{\text{Na}}^0} = \frac{\eta_{\text{Na}}}{\frac{D_{\text{Ca}}}{D_{\text{Na}}} \eta_M^0 + \eta_{\text{Na}}^0}. \quad (9)$$

Both of these depend on the diffusion coefficient ratio $D_{\text{Ca}} / D_{\text{Na}}$. We choose this ratio to be 0.1, reflecting the relative difficulty Ca^{2+} has diffusing within the “stew” of oxygens in the selectivity filter. This is the value we have used in the past [13, 15, 25] and is consistent with similar models of ryanodine receptor calcium channels that reproduce experimental data [16-19].

While different values will scale the heights of the curves in Fig. 4, qualitatively the results will be the same. Fig. 4 shows that both Ca^{2+} and Na^+ contribute substantially to the total conductance. Counterintuitively, even with 10 mM Ca^{2+} and micromolar Gd^{3+} in the baths, Na^+ is still present in both the selectivity filter and the vestibules and therefore still contributes to the

conductance (Fig. 5A). Its concentration in the selectivity filter is reduced ~ 30 fold compared to no Ca^{2+} or Gd^{3+} in the baths [15], but it has not been completely displaced yet in the conditions we consider. Ca^{2+} conductance is similar to Na^+ conductance because $\eta_{\text{Ca}} > \eta_{\text{Na}}$ (due high Ca^{2+} in the filter, Fig. 5B), but $D_{\text{Ca}} / D_{\text{Na}}$ is small.

Effect of Gd^{3+} concentration on permeant ions

Because the normalized total conductance γ / γ^0 is determined by the binding selectivity of the pore for Na^+ and the divalents M^{2+} , we examine the effect $[\text{Gd}^{3+}]$ has on the distributions of these ions within the pore. Fig. 5 shows the concentration profiles of Na^+ , M^{2+} , and Gd^{3+} as Gd^{3+} is added. These show the general behavior of ion binding that have been shown in other studies of this model pore [12, 13, 15, 22, 25]. For example, the high-valence ions like the divalents bind preferentially in the center of the pore with smaller, secondary accumulation sites (“binding sites”) just outside the selectivity filter. In contrast, Na^+ also accumulates in the center, but has much higher concentrations in the vestibules. It is important to note that these secondary binding sites (similar to those postulated in chemical kinetics models [26]) are not built into the model. Rather, they are a natural result of the physics put into the model pore, namely ions of finite size (not point charges) competing for space in a crowded selectivity filter filled with negatively-charged, flexible side chains. For example, the large peaks of Na^+ accumulation outside the selectivity filter show that it is more energetically favorable for Na^+ to screen the charge of the selectivity filter from the outside, rather than find space in the crowded filter. The divalents, on the other hand, can screen the glutamates more efficiently than the Na^+ ions because they take up less volume for the same amount of charge. This balance of electrostatics and excluded volume of the ions (including the glutamate side chains) was first described by Nonner et al. [27] and is called the charge/space competition mechanism (coined by D. Busath in [28]).

As $[\text{Gd}^{3+}]$ increases, the general pattern is the same no matter which divalent M^{2+} is present: the peak of Gd^{3+} in the center of the pore increases, the peak of M^{2+} decreases, filter Na^+ concentration decreases, as do all the ion concentrations in the secondary binding sites in the vestibules. Overall, as Gd^{3+} occupies the center of the pore more often (i.e., with a higher probability), the permeant ions are displaced from both the filter and the vestibules.

Effect of divalent size on Gd³⁺ binding

Despite the general pattern of permeant ions being replaced in the pore by Gd³⁺, there are significant differences in the extent to which the three divalents are displaced from the model pore by increasing [Gd³⁺]. These differences are responsible for the divalent dependence on tonic block shown in Fig. 2. It can be seen that Ba²⁺ is the divalent most easily displaced by Gd³⁺. The concentration profiles in Fig. 5H reveal that even 0.1 μM Gd³⁺ is enough to displace more than half of the Ba²⁺ from the center of the selectivity filter, compared to when no Gd³⁺ is present (compare thick and thin black lines); Na⁺ is also displaced from the entire pore (Fig. 5G). In contrast, 0.1 μM Gd³⁺ has little effect on Ca²⁺ (Fig. 5B) and an intermediate effect on Sr²⁺ (Fig. 5E). For both Ca²⁺ and Sr²⁺, Na⁺ concentration in the pore is little affected by 0.1 μM Gd³⁺ (Figs. 5A and D, respectively).

A different way of looking at the same thing is to consider the number of each cation (Na⁺, M²⁺, and Gd³⁺) in the selectivity filter. Fig. 6 shows these filter occupancies as [Gd³⁺] is increased. Each panel shows a different cation (A: Gd³⁺; B: Na⁺; C: M²⁺) when different divalents are present (solid lines: Ca²⁺; dashed lines: Sr²⁺; dotted lines: Ba²⁺). The figure shows that Ca²⁺ competes best with Gd³⁺ for the selectivity filter: the Gd³⁺ occupancy curve when Ca²⁺ is present (Fig. 6A, solid curve) is to the right of both the Sr²⁺ and Ba²⁺ curves (Fig. 6A, dashed and dotted curves, respectively). Similarly, when Ca²⁺ is present, both the Na⁺ occupancy curve (Fig. 6B, solid line) and the Ca²⁺ occupancy curves (Fig. 6C, solid line) are to the right of the same curves when either Sr²⁺ or Ba²⁺ are present (Fig. 6B and C, dashed and dotted curves, respectively); it takes relatively little Gd³⁺ to displace the permeant cations when Ba²⁺ is present, more Gd³⁺ when Sr²⁺ is present, and even more when Ca²⁺ is present.

DISCUSSION

Charge/space competition

The pattern of ion binding selectivity found in the tonic block experiments (Fig. 2) is consistent with the L-type calcium channel's tendency to be more selective for small ions (with the notable exception not considered here that Mg²⁺ is not preferred over the larger Ca²⁺, presumably due to ion dehydration effects [29]). In this case, the selectivity sequence Ca²⁺>Sr²⁺>Ba²⁺ mirrors ion size: Ca²⁺ is smallest (radius 0.95 Å) and Ba²⁺ largest (radius 1.35 Å), with Sr²⁺ of intermediate size (radius 1.13 Å).

In modeling the L-type channel to define its selectivity mechanism, we and our co-workers have found that this channel selects ions by the charge/space competition mechanism [12-15, 22, 23, 25, 30], as do other Ca^{2+} selective pores like the ryanodine receptor calcium channel [16-19], mutated and chemically modified OmpF porins [31-33], and negatively-charged synthetic nanopores [34, 35]. The pattern of cations being replaced in the pore by Gd^{3+} —with the smaller Ca^{2+} competing much more effectively with Gd^{3+} than the larger Sr^{2+} and Ba^{2+} —is consistent with the charge/space competition mechanism of selectivity. In this mechanism, selectivity is determined by a balance of protein charges attracting the cations into the selectivity filter and of the ions finding space in a selectivity filter where $\sim 25\%$ of the available space is taken up by the eight oxygens of the four glutamate side chains. In such a crowded environment it takes less free energy to insert a Ca^{2+} ion than a Ba^{2+} ion because the Ca^{2+} ion has $\sim 40\%$ of the volume of the Ba^{2+} ion; the entropy change is less when a smaller ion is inserted. For both these divalents, even less energy is required to insert a Gd^{3+} ion because it has more charge. Therefore, as $[\text{Gd}^{3+}]$ increases, it is more likely that a Gd^{3+} enters the pore. However, Gd^{3+} requires more energy to remove a Ca^{2+} from the pore than a Ba^{2+} because of Ca^{2+} 's relative stability over Ba^{2+} .

As for the change in conductance, we find that Gd^{3+} does not permeate the model pore. This is because Gd^{3+} binds with any appreciable concentration only in the center of the selectivity filter, which creates regions of high resistance to Gd^{3+} current flow elsewhere; the low-concentration regions (depletion zones) have high resistance just like any low-concentration electrolyte solution, as described previously [13, 34, 36]. When Gd^{3+} is in the filter, then the permeant cations Na^+ and the divalents M^{2+} do not occupy the pore and therefore do not produce a current.

But, Gd^{3+} is not always in the pore; it has a probability of being in the selectivity filter that depends on $[\text{Gd}^{3+}]$. When Gd^{3+} is not in the pore, then Na^+ and the divalents M^{2+} can conduct through the channel. The calculated current is then a long-time statistical average of this process. Therefore, the reduction of current comes about as the probability of Gd^{3+} being in the selectivity filter increases with $[\text{Gd}^{3+}]$, blocking permeant ion current more and more of the time.

This explanation of current reduction is similar to what has been proposed for Ca^{2+} block of monovalent current [13, 19, 36] (i.e., the classic Ca^{2+} versus Na^+ anomalous mole fraction effect found by Almers, McCleskey, and Palade [1, 2]). Like Gd^{3+} , Ca^{2+} (and other divalents)

occupy the center of the selectivity filter, blocking monovalent current during that time. However, Ca^{2+} is not bound as tightly in the pore as Gd^{3+} and can be displaced by another Ca^{2+} often enough to make an appreciable Ca^{2+} current. Considered in terms of resistors in an equivalent circuit, Ca^{2+} has relatively low resistance in the selectivity filter where its concentration is high, but very high resistance everywhere else because its concentration is low there. Ca^{2+} conductance through the entire pore is low—despite its high occupancy in the selectivity filter—because these resistors are in series. The same principle has recently also been demonstrated in the ryanodine receptor calcium channel [19].

That the model reproduces the experimental data of tonic block is encouraging, but not proof that the model is correct. However, the model has also reproduced a great deal of experimental data of the L-type calcium channel (described in Theory and Methods). Moreover, in the tonic block experiments shown in Fig. 2, there are three cations competing for the pore, and to our knowledge this is the first ion channel model to reproduce experiments for such a challenging case. Taken collectively, the model of the L-type calcium channel we use here seems to capture the dominant physics of selectivity.

Implications for tonic block

The implications of this study are that tonic block is due to the block of permeant cation current by Gd^{3+} because Gd^{3+} competes with these cations for the selectivity filter. Our study indicates that changes in open probability are not needed to explain tonic block. This view is consistent with the view of Babich et al., which was developed after a large number of experiments [5]. We cannot definitively rule out some changes in gating, but in the model the Gd^{3+} dependence of changes in current can—to first order—be explained by the three cations competing for the selectivity filter.

Babich et al. suggest that the place where the competition occurs is not the selectivity filter, but rather at the entrance of the permeation pathway (but still admitting that the actual location is unknown). Moreover, they suggest that the binding of Gd^{3+} can occur when the channel is closed. Our very reduced model pore only includes the selectivity filter and uncharged vestibules, and it only describes an open channel. Therefore, we cannot say definitively if their view is correct. However, suppose that their view is correct and that the competition of ions occurs at a binding site extracellular to the selectivity filter when the channel is closed. When the channel does open and inward current flows (as in the tonic block

experiments), those ions will move into the selectivity filter where the competition we describe must occur because, by definition, the selectivity filter has the highest affinity for cations. Therefore, while the competitive ion binding that occurs when the channel is closed may happen in another location, the competition that is reflected in the measured current is the one that happens in the selectivity filter.

Prediction of the model

The model indicates that tonic block by Gd^{3+} is due to competitive ion binding in the selectivity filter. In this view, Gd^{3+} competes away the divalents and Na^+ from the selectivity filter as $[\text{Gd}^{3+}]$ increases. However, the charge/space competition mechanism also predicts that the other cations can compete away Gd^{3+} from the pore. For example, this model of the L-type channel has predicted a Na^+ concentration dependence of Ca^{2+} block [15]; a similar prediction in the ryanodine receptor calcium channel was experimentally verified [19].

For the tonic block considered here, we propose a Ca^{2+} concentration dependence of Gd^{3+} block. In Fig. 7 we show how increasing $[\text{Ca}^{2+}]$ to 100 mM can change tonic block; $\sim 100 \mu\text{M}$ Gd^{3+} is required to decrease the conductance by half, as compared to $\sim 1 \mu\text{M}$ Gd^{3+} for 10 mM Ca^{2+} . On the other hand, having only 1 mM Ca^{2+} makes it easier for Gd^{3+} to occupy the pore, with 50% conductance reduction at only $\sim 0.1 \mu\text{M}$ Gd^{3+} .

We are not currently equipped to validate this prediction, but we hope to do so in future work. As with the results shown in Fig. 2, it is probable that the model results will only be qualitatively accurate. However, the model's qualitative predictions are clear: there is competitive binding in the pore so that there is a large dependence of current on $[\text{Ca}^{2+}]$. Specifically, for a 10 fold increase in $[\text{Ca}^{2+}]$ from 10 mM to 100 mM, the IC_{50} 's change ~ 100 fold, but for a 10 fold increase in $[\text{Ca}^{2+}]$ from 1 mM to 10 mM, the IC_{50} 's change only ~ 10 fold.

CONCLUSION

Trivalent cations alter the permeation and gating properties of calcium channels in general [7, 37, 38], making them useful laboratory tools [39-41]. In fact, trivalents affect many kinds of ion channels (e.g., [42, 43]). Here we described a possible mechanism for one of these effects on calcium channels (tonic block). Specifically, we showed that tonic block's reduction of Na^+ and divalent currents by increasing $[\text{Gd}^{3+}]$ can be described by these ions competitively binding within the selectivity filter. This supports the view of Babich et al. [5] that tonic block

does not reflect changes in the channel's gating properties and is in this way distinctly different from use-dependent block. Our results also give further evidence that selectivity in the L-type calcium channel stems from a balance of electrostatic attraction of cations into the filter and excluded volume repulsion of the ions from the crowded filter (charge/space competition).

ACKNOWLEDGMENTS

The authors are grateful to Daphne Atlas for drawing their attention to the role of trivalent ions in calcium channels. We also thank Roman Shirokov for useful discussions about the experiments. Computer time by the Ira and Marylou Fulton Supercomputing Center at Brigham Young University is gratefully acknowledged. DB was supported by the Hungarian National Research Fund (OTKA K75132). MV is grateful for the support of the Hungarian National Research Fund (OTKA K68641) and the Janos Bolyai Research Fellowship. DH and DB were supported in part by NIH grant GM076013 (Bob Eisenberg, PI). We thank Wolfgang Nonner and Bob Eisenberg for comments on the manuscript.

REFERENCES

- [1] W. Almers, E.W. McCleskey, P.T. Palade, A non-selective cation conductance in frog muscle membrane blocked by micromolar external calcium ions, *J. Physiol. (London)* 353 (1984) 565-583.
- [2] W. Almers, E.W. McCleskey, Non-selective conductance in calcium channels of frog muscle: calcium selectivity in a single-file pore, *J. Physiol. (London)* 353 (1984) 585-608.
- [3] B.A. Biagi, J.J. Enyeart, Gadolinium blocks low- and high-threshold calcium currents in pituitary cells, *Am J Physiol Cell Physiol* 259 (1990) C515-520.
- [4] A. Lacampagne, F. Gannier, J. Argibay, D. Garnier, J.-Y. Le Guennec, The stretch-activated ion channel blocker gadolinium also blocks L-type calcium channels in isolated ventricular myocytes of the guinea-pig, *Biochimica et Biophysica Acta (BBA) - Biomembranes* 1191 (1994) 205-208.
- [5] O. Babich, J. Reeves, R. Shirokov, Block of $\text{Ca}_v1.2$ channels by Gd^{3+} reveals preopening transitions in the selectivity filter, *J. Gen. Physiol.* 129 (2007) 461-475.
- [6] J.B. Lansman, Blockade of current through single calcium channels by trivalent lanthanide cations. Effect of ionic radius on the rates of ion entry and exit, *J. Gen. Physiol.* 95 (1990) 679-696.
- [7] C.A. Obejero-Paz, I.P. Gray, S.W. Jones, Y^{3+} block demonstrates an intracellular activation gate for the $\alpha 1\text{G}$ T-type Ca^{2+} channel, *J. Gen. Physiol.* 124 (2004) 631-640.
- [8] K.E. Cooper, P.Y. Gates, R.S. Eisenberg, Diffusion theory and discrete rate constants in ion permeation, *J. Membr. Biol.* 106 (1988) 95-105.
- [9] R.S. Eisenberg, Computing the field in proteins and channels., *J. Membr. Biol.* 150 (1996) 1-25.
- [10] W. Nonner, B. Eisenberg, Ion permeation and glutamate residues linked by Poisson-Nernst-Planck theory in L-type calcium channels, *Biophys. J.* 75 (1998) 1287-1305.
- [11] W. Nonner, D.P. Chen, B. Eisenberg, Progress and Prospects in Permeation, *J. Gen. Physiol.* 113 (1999) 773-782.
- [12] D. Boda, M. Valiskó, B. Eisenberg, W. Nonner, D. Henderson, D. Gillespie, Combined effect of pore radius and protein dielectric coefficient on the selectivity of a calcium channel, *Phys. Rev. Lett.* 98 (2007) 168102.

- [13] D. Gillespie, D. Boda, The anomalous mole fraction effect in calcium channels: A measure of preferential selectivity, *Biophys. J.* 95 (2008) 2658-2672.
- [14] D. Boda, W. Nonner, D. Henderson, B. Eisenberg, D. Gillespie, Volume exclusion in calcium selective channels, *Biophys. J.* 94 (2008) 3486-3496.
- [15] D. Boda, M. Valiskó, D. Henderson, B. Eisenberg, D. Gillespie, W. Nonner, Ionic selectivity in L-type calcium channels by electrostatics and hard-core repulsion, *J. Gen. Physiol.* 133 (2009) 497-509.
- [16] D. Gillespie, L. Xu, Y. Wang, G. Meissner, (De)constructing the ryanodine receptor: Modeling ion permeation and selectivity of the calcium release channel, *J. Phys. Chem. B* 109 (2005) 15598-15610.
- [17] D. Gillespie, Energetics of divalent selectivity in a calcium channel: the ryanodine receptor case study, *Biophys. J.* 94 (2008) 1169-1184.
- [18] D. Gillespie, M. Fill, Intracellular calcium release channels mediate their own countercurrent: The ryanodine receptor case study, *Biophys. J.* 95 (2008) 3706-3714.
- [19] D. Gillespie, J. Giri, M. Fill, Reinterpreting the anomalous mole fraction effect: The ryanodine receptor case study, *Biophys. J.* 97 (2009) 2212-2221
- [20] J. Yang, P.T. Ellinor, W.A. Sather, J.-F. Zhang, R. Tsien, Molecular determinants of Ca^{2+} selectivity and ion permeation in L-type Ca^{2+} channels., *Nature* 366 (1993) 158-161.
- [21] P.T. Ellinor, J. Yang, W.A. Sather, J.-F. Zhang, R. Tsien, Ca^{2+} channel selectivity at a single locus for high-affinity Ca^{2+} interactions, *Neuron* 15 (1995) 1121-1132.
- [22] D. Boda, M. Valiskó, B. Eisenberg, W. Nonner, D. Henderson, D. Gillespie, The effect of protein dielectric coefficient on the ionic selectivity of a calcium channel, *J. Chem. Phys.* 125 (2006) 034901.
- [23] D. Boda, D. Henderson, D.D. Busath, Monte Carlo study of the selectivity of calcium channels: Improved geometry, *Mol. Phys.* 100 (2002) 2361-2368.
- [24] A. Malasics, D. Gillespie, D. Boda, Simulating prescribed particle densities in the grand canonical ensemble using iterative algorithms, *J. Chem. Phys.* 128 (2008) 124102.
- [25] A. Malasics, D. Gillespie, W. Nonner, D. Henderson, B. Eisenberg, D. Boda, Protein structure and ionic selectivity in calcium channels: Selectivity filter size, not shape, matters, *Biochimica et Biophysica Acta (BBA) - Biomembranes* in press (2009).

- [26] W.A. Sather, E.W. McCleskey, Permeation and selectivity in calcium channels, *Annu. Rev. Physiol.* 65 (2003) 133-159.
- [27] W. Nonner, L. Catacuzzeno, B. Eisenberg, Binding and selectivity in L-type calcium channels: A mean spherical approximation, *Biophys. J.* 79 (2000) 1976-1992.
- [28] D. Boda, D.D. Busath, D. Henderson, S. Sokolowski, Monte Carlo simulations of the mechanism of channel selectivity: The competition between volume exclusion and charge neutrality, *J. Phys. Chem. B* 104 (2000) 8903-8910.
- [29] W. Nonner, D. Gillespie, D. Henderson, B. Eisenberg, Ion accumulation in a biological calcium channel: effects of solvent and confining pressure, *J. Phys. Chem. B* 105 (2001) 6427-6436.
- [30] D. Boda, D. Henderson, D.D. Busath, Monte Carlo study of the effect of ion and channel size on the selectivity of a model calcium channel, *J. Phys. Chem. B* 105 (2001) 11574-11577.
- [31] H. Miedema, A. Meter-Arkema, J. Wierenga, J. Tang, B. Eisenberg, W. Nonner, H. Hektor, D. Gillespie, W. Meijberg, Permeation properties of an engineered bacterial OmpF porin containing the EEEE-Locus of Ca²⁺ channels, *Biophys. J.* 87 (2004) 3137-3147.
- [32] M. Vrouenraets, J. Wierenga, W. Meijberg, H. Miedema, Chemical Modification of the Bacterial Porin OmpF: Gain of Selectivity by Volume Reduction, *Biophys. J.* 90 (2006) 1202-1211.
- [33] H. Miedema, M. Vrouenraets, J. Wierenga, D. Gillespie, B. Eisenberg, W. Meijberg, W. Nonner, Ca²⁺ selectivity of a chemically modified OmpF with reduced pore volume, *Biophys. J.* 91 (2006) 4392-4400.
- [34] D. Gillespie, D. Boda, Y. He, P. Apel, Z.S. Siwy, Synthetic nanopores as a test case for ion channel theories: The anomalous mole fraction effect without single filing, *Biophys. J.* 95 (2008) 609-619.
- [35] Y. He, D. Gillespie, D. Boda, I. Vlassiuk, R.S. Eisenberg, Z.S. Siwy, Tuning transport properties of nanofluidic devices with local charge inversion, *J. Am. Chem. Soc.* 131 (2009) 5194-5202.
- [36] W. Nonner, D.P. Chen, B. Eisenberg, Anomalous mole fraction effect, electrostatics, and binding in ionic channels, *Biophys. J.* 74 (1998) 2327-2334.

- [37] R. Vennekens, J. Prenen, J.G.J. Hoenderop, R.J.M. Bindels, G. Droogmans, B. Nilius, Pore properties and ionic block of the rabbit epithelial calcium channel expressed in HEK 293 cells, *The Journal of Physiology* 530 (2001) 183-191.
- [38] S. Sárközi, C. Szegedi, B. Lukács, M. Ronjat, I. Jóna, Effect of gadolinium on the ryanodine receptor/sarcoplasmic reticulum calcium release channel of skeletal muscle, *FEBS Journal* 272 (2005) 464-471.
- [39] I. Lerner, M. Trus, R. Cohen, O. Yizhar, I. Nussinovitch, D. Atlas, Ion interaction at the pore of Lc-type Ca^{2+} channel is sufficient to mediate depolarization-induced exocytosis, *J. Neurochem.* 97 (2006) 116-127.
- [40] M. Trus, R.F. Corkey, R. Nesher, A.-M.T. Richard, J.T. Deeney, B.E. Corkey, D. Atlas, The L-type voltage-gated Ca^{2+} channel is the Ca^{2+} sensor protein of stimulus-secretion coupling in pancreatic beta Cells, *Biochemistry* 46 (2007) 14461-14467.
- [41] R.A. Bannister, I.N. Pessah, K.G. Beam, The skeletal L-type Ca^{2+} current is a major contributor to excitation-coupled Ca^{2+} entry, *J. Gen. Physiol.* 133 (2008) 79-91.
- [42] C.M. Armstrong, G. Cota, Modification of sodium channel gating by lanthanum. Some effects that cannot be explained by surface charge theory, *J. Gen. Physiol.* 96 (1990) 1129-1140.
- [43] X.C. Yang, F. Sachs, Block of stretch-activated ion channels in *Xenopus* oocytes by gadolinium and calcium ions, *Science* 243 (1989) 1068-1071.

FIGURE LEGENDS

1. Geometry of the model pore. At left, a cross section of the pore is shown. The baths and simulations cell are several times larger than shown here. At right, the selectivity filter containing the eight oxygens (large (red) spheres) is shown in a simulation snapshot. Also, in the filter are one Ca^{2+} (green sphere) and one Na^+ (blue sphere). The region of confinement of the oxygens ($-5 < z < 5 \text{ \AA}$) is shown with the span of the arrows.
2. Comparison of the normalized conductances from experiments (large, solid symbols) to those computed from the model (small, open symbols). The lines are fits of the model results to Eq. (5). In the simulations, there is 150 mM NaCl, the indicated amount of GdCl_3 , and 10 mM divalent cation: Ca^{2+} solid (black) curve and square (black) symbols; Sr^{2+} dashed (red) curve and circle (red) symbols; Ba^{2+} dotted (blue) curve and triangle (blue) symbols.
3. The line density profile ratio $n_{\text{Ca}}(z)/n_{\text{Na}}(z)$ at different $[\text{Gd}^{3+}]$. The results with Sr^{2+} and Ba^{2+} are qualitatively identical.
4. Individual normalized ion conductances at different $[\text{Gd}^{3+}]$. The lines are fits of simulation results to Eq. (5). The total conductance is thick (black) line, Na^+ conductance the thin (red) line, and Ca^{2+} the dashed (blue) line.
5. Concentration profiles of ions in the pore: top row (A, D, G) Na^+ ; middle row (B, E, H) divalent M^{2+} ; bottom row (C, F, I) Gd^{3+} . The left column (A, B, C) are when the divalent is Ca^{2+} , the middle column (D, E, F) Sr^{2+} , and the right column (G, H, I) Ba^{2+} . The thick black line is when $[\text{Gd}^{3+}] = 0$, the thin black line when $[\text{Gd}^{3+}]$ is 0.1 μM , the long-dashed (red) line when $[\text{Gd}^{3+}]$ is 1 μM , and the dotted (blue) line when $[\text{Gd}^{3+}]$ is 10 μM . These concentrations are given in molar instead of the line density used in Eq. (2). The area used to compute this molar concentration from the line density is the cross-sectional area accessible to the center of each ion species.
6. Occupancy of each cation species in the selectivity filter ($-5 \text{ \AA} < z < 5 \text{ \AA}$ in Fig. 1) when different divalents are present: Ca^{2+} solid (black) curves and square (black) symbols; Sr^{2+} dashed (red) curves and circle (red) symbols; Ba^{2+} dotted (blue) curves and triangle (blue) symbols. (A) The number of Gd^{3+} in the filter. (B) Na^+ . (C) divalents M^{2+} .

7. A prediction of the model for Ca^{2+} concentration dependence of tonic block. Three different Ca^{2+} concentrations are shown: 1 mM, black line and square symbols; 10 mM, red line and circle symbols; 100 mM, blue line and triangle symbols. The 10 mM case is the same as in Fig. 2 for comparison. In each case, $[\text{Na}^+]$ is 150 mM and Gd^{3+} is added. The lines are fits to Eq. (5) with IC_{50} 's of 0.12 μM for 1 mM Ca^{2+} , 1.6 μM for 10 mM, and 120 μM for 100 mM.

Figure 1

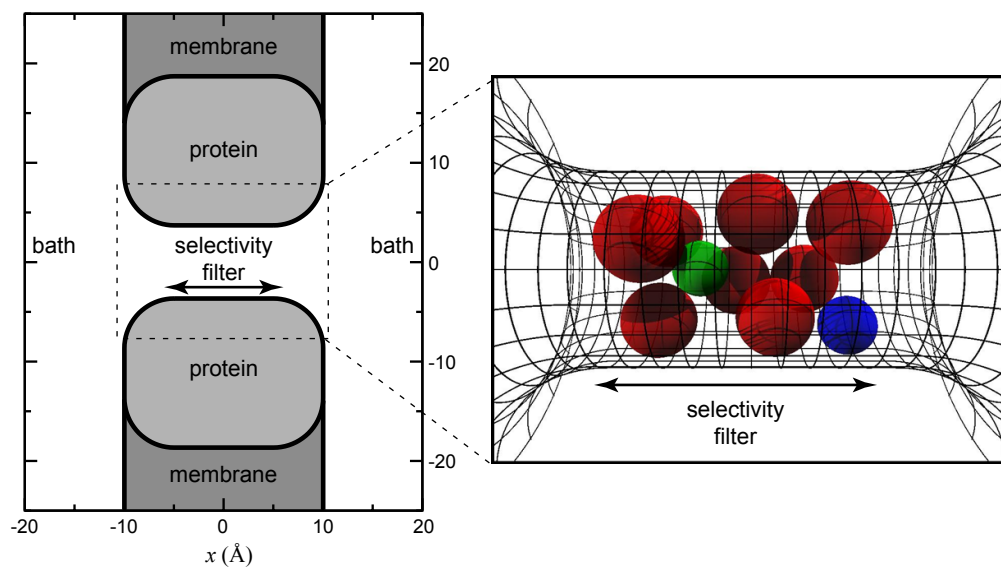


Fig. 1

Figure 2

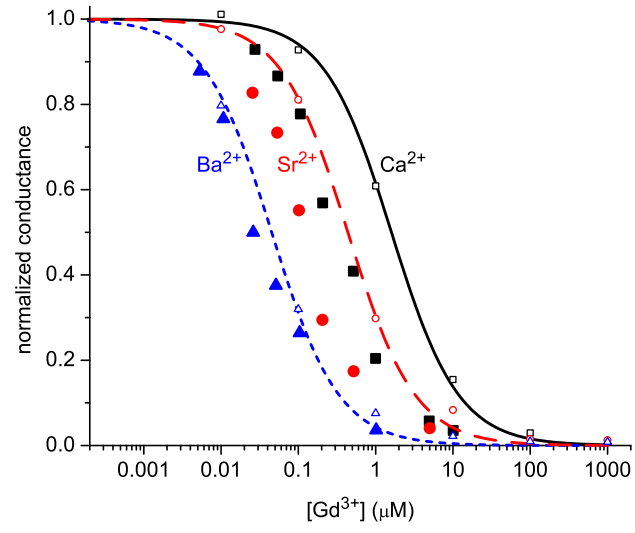


Fig. 2

Figure 3

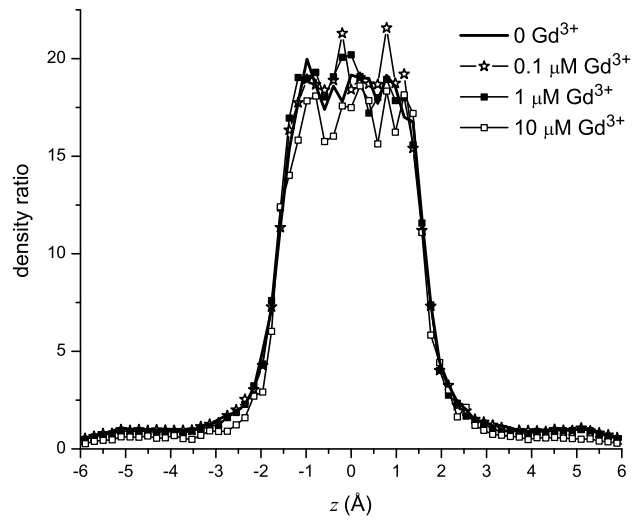


Fig. 3

Figure 4

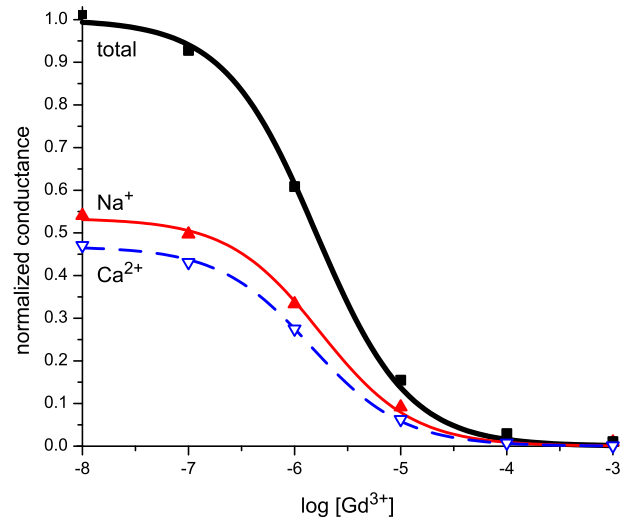


Fig. 4

Figure 5

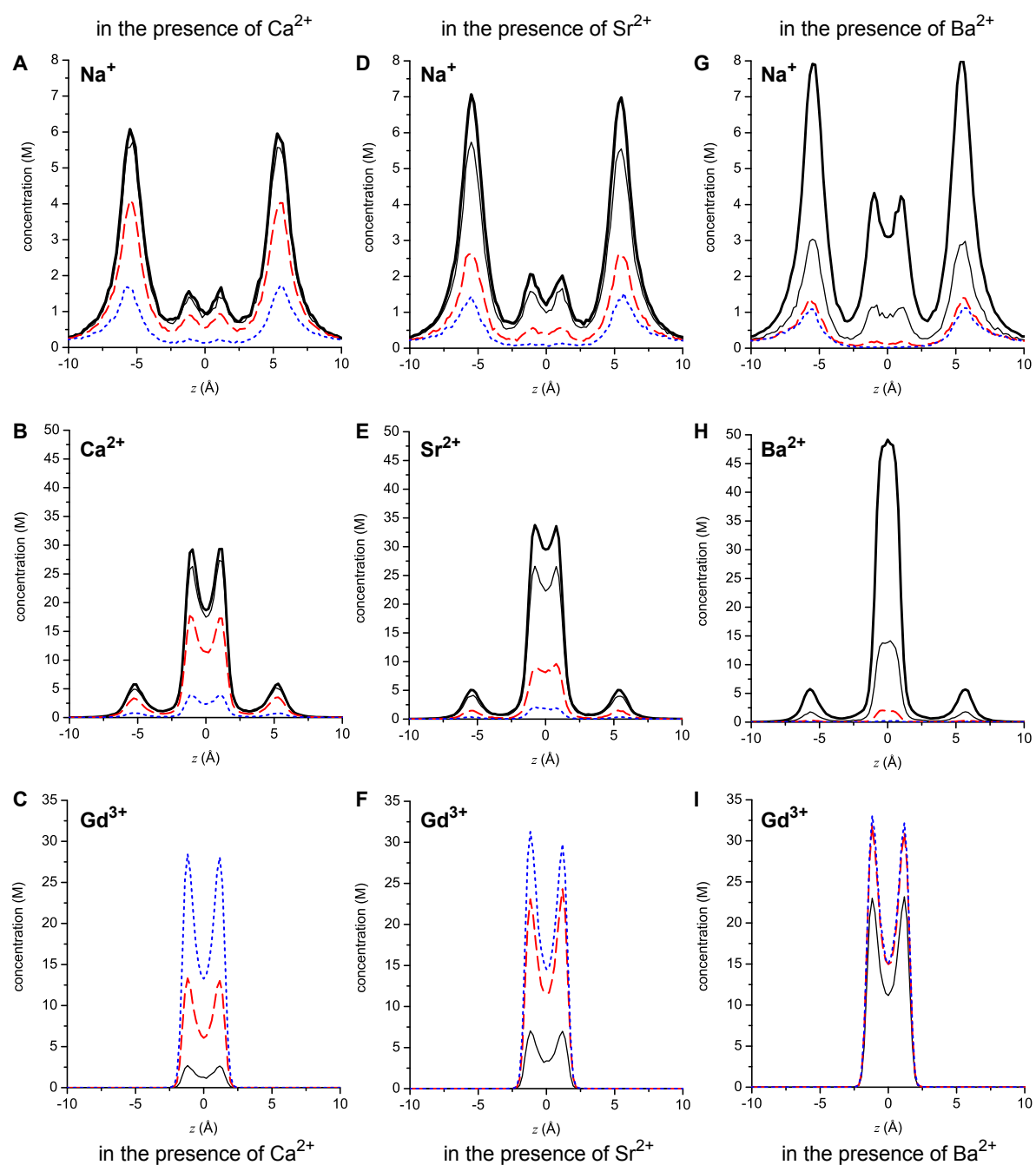


Fig. 5

Figure 6

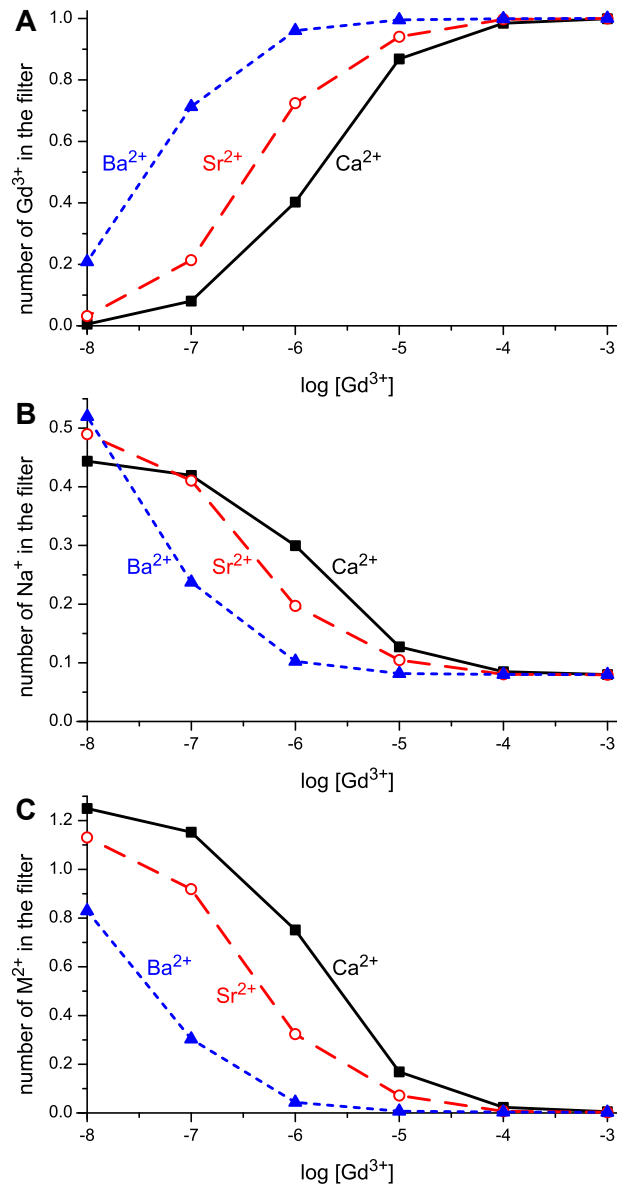


Fig. 6

Figure 7

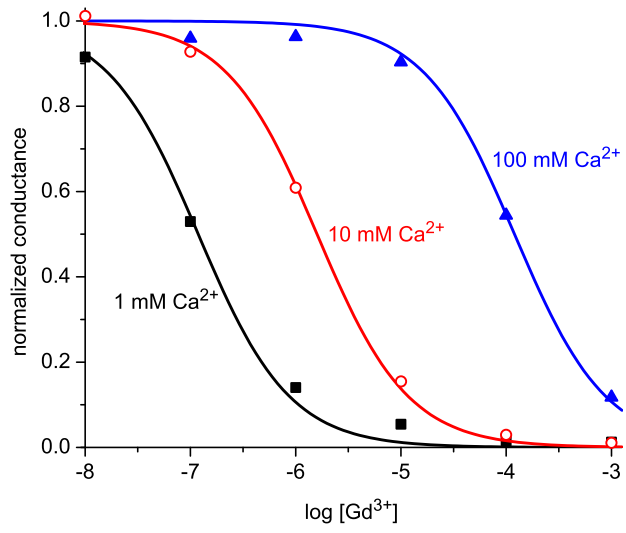


Fig. 7